

Optical qubit by conditional interferometry

Matteo G. A. Paris*

*Optics Section, Blackett Laboratory, Imperial College, London SW7 2BZ, United Kingdom
and Dipartimento "A. Volta" and Unitá INFN, Università di Pavia, via Bassi 6, I-27100 Pavia, Italy*

(Received 24 September 1999; published 15 August 2000)

We suggest a method to prepare any chosen superposition $a_0|0\rangle + a_1|1\rangle$ of the vacuum and one-photon states. The method is based on a conditional double interferometer fed by a one-photon state and a coherent state. The scheme involves only linear optical elements and avalanche photodetectors, and therefore it should be realizable with current technology. A realistic description of the triggering photodetectors is employed, i.e., we assume that they can only check, with a certain efficiency, whether or not any photon is present. We discuss two working regimes, and show that output states with fidelity arbitrarily close to unit may be obtained, with nonvanishing conditional probability, also for low quantum efficiency at the photodetectors.

PACS number(s): 42.50.Dv, 03.65.Bz

I. INTRODUCTION

The past two decades have witnessed a substantial development in quantum engineering and measurement of light. Several kinds of nonclassical states of light can now be generated, and their quantum properties can be fully characterized by accessible measurement schemes [1,2]. Besides fundamental interest, nonclassical states also find applications, as, for example, the use of number states in quantum communication channels, and of squeezed light in high-precision gyroscopes and interferometers. More recently, the quantum engineering of light received new attention, which is mainly motivated by the potential improvement offered by quantum mechanics to the manipulation and the transmission of information [3]. Indeed, phenomena such as teleportation [4] and quantum dense coding [5] found their first implementation in the quantum optical domain.

Photons do not interact, and this feature is very useful for the transmission of information without signal degradation. Indeed, the typical figures for losses in optical fibers are below 0.3 dB/Km. On the other hand, the same characteristic poses limitations to the manipulation of the quantum information encoded into a quantum state of light. Photon-photon interactions needed for computation, in fact, take place only in active optical media, characterized by nonlinear susceptibility. Usually, such nonlinearities are small, or masked by the concurrent absorption processes. Only recently, new methods based on dark atomic resonance and electromagnetically induced transparency [6] have been suggested to strongly enhance nonlinearity while suppressing absorption. The possibility of such giant nonlinearities renewed the interest for optical quantum technology, as it opens new perspectives to build single-photon quantum logic gates.

In this paper, we devote our attention to the preparation of any chosen superposition of the vacuum and the one-photon states $a_0|0\rangle + a_1|1\rangle$. This is the simplest state of light that carries a complete phase information, and, in turn, it represents the simplest example of an optical qubit. Remarkably, this is a low-energy-expense encoding of quantum informa-

tion, as it requires, on average, less than one photon for each qubit. In particular, for the conventional computational basis $|\psi_{\pm}\rangle = 1/\sqrt{2}[|0\rangle \pm |1\rangle]$, i.e., for balanced superposition, half a photon for each qubit is required.

Different methods have been discussed with the purpose of engineering superpositions of radiation states. Mostly, these are in the context of cavity QED, since the interaction with atoms passing through the cavity allows us to select specific components of an initial signal [7]. More recently, an all-optical device, based a ring cavity coupled to the signal through a Kerr medium, has been suggested to realize Fock filtering, and thus preparation of superpositions [8]. In addition, a conditional scheme based on beam splitters and conditional zero counters has been suggested to produce an arbitrary superposition [9], however without investigating the effects of the imperfections of photodetectors. Finally, a scheme to implement the optical state truncation [10] of a coherent state has been proposed, which, in turn, is used to prepare superpositions. As we will see, this last setup corresponds to a particular case of the present proposal.

The present scheme involves only linear optical elements and avalanche photodetectors, and therefore it should be realizable with current technology. In essence, it consists of two Mach-Zehnder interferometers arranged such that one of the outputs from the first one is then used as input for the second one. The first MZ is fed by a one-photon state, whereas the second is fed by a weak coherent state. The output states of the second interferometers are then measured, and the conditional output state from the first MZ turns out to be a superposition of the vacuum and one-photon states. The amplitudes for the two components can be tuned by varying the internal phase shifts of the two interferometers and the amplitude of the coherent input.

The paper is structured as follows. In the next section the scheme is presented and its dynamics is evaluated. Then, the ideal conditional output state is calculated for the case of a perfect photodetection process. In Sec. III we take into account the imperfections of realistic photodetectors, and study their effects on the preparation of the superposition. In the literature two models of photodetectors (PDs) have been employed. In the first, which we use throughout the paper, it is assumed that PDs are only able to check, with a certain ef-

*Email address: paris@unipv.it

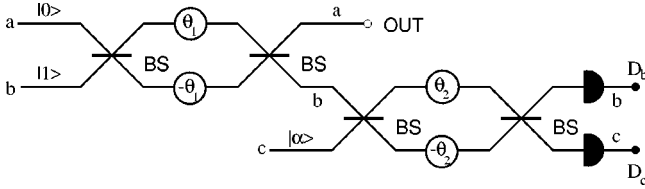


FIG. 1. Schematic diagram of the conditional interferometric setup for the preparation of any chosen superposition $a_0|0\rangle + a_1|1\rangle$ of the vacuum and one-photon states. The BS are identical balanced beam splitters, whereas D_b and D_c denote two identical avalanche photodetectors. The first stage consists of a Mach-Zehnder interferometer fed by a one-photon state in mode b . Then, one of the outputs from the first interferometer is used as an input of the other one, whose second port (mode c) is excited in a weak coherent state. Both the output modes from the second interferometer are detected by avalanche photodetectors, and depending on the observed result we obtain a different conditional output state in the mode a (denoted by OUT in the picture). The event of recording one photon in one of the photodetectors (either D_b or D_c) and no photons in the other one corresponds to the preparation of a superposition of the vacuum and one-photon states. The relative weights of the two components may be tuned by varying either the internal phase shifts θ_1 and θ_2 or the amplitude $|\gamma\rangle$ of the coherent input, whereas the phase of superposition equals the argument $\arg\gamma$.

efficiency, whether or not photons are present. This is a reliable description of customary avalanche photodetectors, and we refer to this as YES/NO photodetection. In the second model, PDs are still affected by nonunit quantum efficiency, but now they are able to discriminate among the number of incoming photons, thus acting as photocounters. This description does not yet correspond to available PDs, as no evidence of detectors capable of discriminating between the presence of, say, n and $n+1$ photons for a generic n has been reported. The photocounter model has been sometimes used in the literature on conditional measurements, for instance in Ref. [10], and this led to the conclusion that schemes are reasonably insensitive to the detectors' inefficiency. In general, this is no longer true when the realistic features of avalanche photodetectors are taken into account. On the other hand, we will show that the present scheme offers a working regime in which the use of YES/NO detectors is enough to assure the reliable preparation of any chosen superposition. Finally, Sec. IV closes the paper by discussing and summarizing results.

II. CONDITIONAL DOUBLE INTERFEROMETRY

The scheme we have in mind is the conditional double interferometer depicted in Fig. 1. It consists of two Mach-Zehnder interferometers in cascade, in a way that causes one of the output signals from the first one to constitute one of the input signals for the second one. The three field modes involved in the setup are denoted by a, b , and c , whereas the BS's are symmetric beam splitters. We also assume that equal and opposite phase shifts, denoted by θ_1 and θ_2 , respectively, are imposed in the arms of each interferometer (see Fig. 1). We assume that the two interferometers are built with identical balanced beam splitters, and this means that

they are fully characterized by the value of the internal phase-shift between their arms. The first interferometer is fed by a one-photon state in the mode b , whereas the other port, corresponding to mode a , is left unexcited. After this first stage the photon has a nonzero amplitude of being in both the output paths, whereas the values of such amplitudes are determined by the internal phase shift θ_1 . The output mode b is then mixed with mode c , prepared in a weak coherent state $|\gamma\rangle$, and they are both detected at the output of the second interferometer. Depending on the result of the measurements, we have different *conditional* output states for the output mode a of the first interferometer. In particular, we will see that any chosen superposition $a_0|0\rangle + a_1|1\rangle$ of the vacuum and one-photon states can be prepared with nonzero conditional probability.

The evolution operator of each interferometer can be written as

$$\hat{V}_{\text{MZ}}(\theta) = \hat{V}_{\text{BS}} \exp\{i\theta(a^\dagger a - b^\dagger b)\} \hat{V}_{\text{BS}}^\dagger, \quad (1)$$

where

$$\hat{V}_{\text{BS}} = \exp\left\{i\frac{\pi}{4}(a^\dagger b + b^\dagger a)\right\} \quad (2)$$

denotes the evolution operator of a symmetric beam splitter. Equation (1) can be written as

$$\begin{aligned} \hat{V}_{\text{MZ}}(\phi) = & \exp\left\{i\frac{\pi}{2}b^\dagger b\right\} \exp\{-i\phi(a^\dagger b + b^\dagger a)\} \\ & \times \exp\left\{-i\frac{\pi}{2}b^\dagger b\right\}, \end{aligned} \quad (3)$$

which shows that a Mach-Zehnder interferometer is equivalent to a single beam splitter BS_ϕ of transmissivity $\tau = \sin^2\phi$, where $\phi = \theta/2$, preceded and followed by rotations of $\pi/2$ performed on one of the two modes [11]. After straightforward algebra, one may write the evolution operator of the whole device as

$$\begin{aligned} \hat{U}(\phi_1, \phi_2) = & \exp\left\{i\frac{\pi}{2}b^\dagger b\right\} \exp\{i\phi_2(b^\dagger c + c^\dagger b)\} \\ & \times \exp\{i\phi_1(a^\dagger b + b^\dagger a)\} \exp\left\{-i\frac{\pi}{2}b^\dagger b\right\}. \end{aligned} \quad (4)$$

The overall input state can be written as

$$|\Psi_{IN}\rangle = |0\rangle_a |1\rangle_b |\gamma\rangle_c, \quad (5)$$

whereas using Eq. (4) we obtain the expression for the overall output,

$$\begin{aligned}
|\Psi_{\text{OUT}}\rangle &= \hat{U}(\phi_1, \phi_2)|\Psi_{\text{IN}}\rangle \\
&= \cos\phi_1|1\rangle_a|\gamma\cos\phi_2\rangle_b|\gamma\sin\phi_2\rangle_c \\
&\quad + \sin\phi_1\sin\phi_2|0\rangle_a b^\dagger|\gamma\cos\phi_2\rangle_b|\gamma\sin\phi_2\rangle_c \\
&\quad - \sin\phi_1\cos\phi_2|0\rangle_a|\gamma\cos\phi_2\rangle_b c^\dagger|\gamma\sin\phi_2\rangle_c.
\end{aligned} \tag{6}$$

We are now ready to analyze the effect on the mode a of a measurement performed on the output modes b and c . For the moment let us assume that the generic measurement of a quantity X on the b mode and Y on the c mode is performed; we also assume that the two quantities are independent of each other. The measurement is thus described by a factorized probability operator measure (POM) $\hat{\Pi} = \hat{\Pi}_x \otimes \hat{\Pi}_y$, where x and y denote the possible outcomes for the two quantities. The POMs are positive (hence self-adjoint) operators. If X and Y denote the spaces of the possible outcomes, the normalization conditions can be written as ($\hat{1}$ denotes the identity operator)

$$\int_X dx \hat{\Pi}_x = \hat{1}, \quad \int_Y dy \hat{\Pi}_y = \hat{1}.$$

The probability of the event (x, y) is given by the global trace over the three modes

$$P_{xy} = \text{Tr}_{abc} [|\Psi_{\text{OUT}}\rangle \langle \Psi_{\text{OUT}}| \hat{\Pi}_x \otimes \hat{\Pi}_y], \tag{7}$$

whereas the corresponding *conditional* output state for the mode a is given by the partial trace

$$\hat{\rho}_{xy} = \frac{1}{P_{xy}} \text{Tr}_{bc} [|\Psi_{\text{OUT}}\rangle \langle \Psi_{\text{OUT}}| \hat{\Pi}_x \otimes \hat{\Pi}_y]. \tag{8}$$

Actually, different measurements on b and c lead to different conditional output states, and since some events are more likely to occur than others, so are the corresponding conditional output states. In the following we consider the measurement of the photon number, and in particular we focus our attention on the case of a single photon recorded in one of the output modes, and no photons recorded in the other one. In order to establish notation, we assume that the photon is recorded in the output mode b . However, the results are valid also for the case of a photon registered in the mode c , up to a $\pi/2$ shift in the internal phase shifts of the second interferometer.

The ideal measurement of the photon number on the two output modes is described by the POM,

$$\hat{\Pi}_{nk} = |n\rangle_{bb}\langle n| \otimes |k\rangle_{cc}\langle k|, \quad n, k = 0, 1, \dots \tag{9}$$

Therefore, the detection probability for the case $n=1, k=0$ is equal to

$$\begin{aligned}
P_{10} &= [\langle \Psi_{\text{OUT}} | 1 \rangle_b | 0 \rangle_c]^2 = e^{-|\gamma|^2} [\sin^2\phi_1 \sin^2\phi_2 \\
&\quad + |\gamma|^2 \cos^2\phi_1 \cos^2\phi_2],
\end{aligned} \tag{10}$$

and the conditional output state for the mode a is given by

$$\begin{aligned}
\hat{\rho}_{10} &= \frac{1}{P_{10}} \text{Tr}_{bc} [|\Psi_{\text{OUT}}\rangle \langle \Psi_{\text{OUT}}| |1\rangle_{bb}\langle 1| \otimes |0\rangle_{cc}\langle 0|] \\
&= \frac{1}{P_{10}} [c_{00}|0\rangle\langle 0| + c_{11}|1\rangle\langle 1| + c_{01}|0\rangle\langle 1| + c_{10}|1\rangle\langle 0|],
\end{aligned} \tag{11}$$

where

$$\begin{aligned}
c_{00} &= e^{-|\gamma|^2} \sin^2\phi_1 \sin^2\phi_2, & c_{11} &= e^{-|\gamma|^2} |\gamma|^2 \cos^2\phi_1 \cos^2\phi_2, \\
c_{01} &= e^{-|\gamma|^2} \gamma \sin\phi_1 \sin\phi_2 \cos\phi_1 \cos\phi_2, & c_{10} &= c_{01}^*,
\end{aligned} \tag{12}$$

the star denoting complex conjugation. By looking at Eqs. (12) it is easy to recognize that $\hat{\rho}_{10}$ is actually a pure state $\hat{\rho}_{10} = |\psi_{10}\rangle\langle\psi_{10}|$, where

$$|\psi_{10}\rangle = \frac{\sin\phi_1 \sin\phi_2 |0\rangle + \gamma \cos\phi_1 \cos\phi_2 |1\rangle}{\sqrt{\sin^2\phi_1 \sin^2\phi_2 + |\gamma|^2 \cos^2\phi_1 \cos^2\phi_2}}. \tag{13}$$

By varying the interferometric shifts and the amplitude γ of the coherent input c , we may achieve any chosen superposition of the vacuum and the one-photon states. In particular, the internal phase shifts ϕ_1 and ϕ_2 , and the modulus $|\gamma|$, govern the weights of the two components, whereas the relative phase equals the argument of the complex amplitude γ .

We notice that the truncation scheme of Ref. [10] is equivalent to a particular case of our setup, corresponding to the balanced choice $\phi_1 = \phi_2 = \pi/4$. This is due, as mentioned above, to the fact that a Mach-Zehnder interferometer is substantially equivalent to a single beam splitter of transmissivity $\tau = \sin^2\phi$. However, besides the fact that the present scheme offers additional degrees of freedom, the use of an interferometric setup has the specific advantage of a larger stability. It should be mentioned that the conditional scheme of [9] requires a smaller number of optical components, however it also shows a smaller detection probability (see below), i.e., a lower efficiency in preparing superpositions.

Remarkably, the superposition of Eq. (13) may be obtained by different values of ϕ_1, ϕ_2 , and γ , and this degree of freedom can be used to maximize the corresponding detection probability P_{10} , i.e., the probability of the event which leaves the state of the mode a into the desired superposition. Let us consider, for example, the preparation of a generic balanced superposition

$$|\psi_\star\rangle = \frac{|0\rangle + e^{i\varphi}|1\rangle}{\sqrt{2}}. \tag{14}$$

In order to reduce Eq. (13) to Eq. (14), we need $\varphi = \arg \gamma$ and $|\gamma| = \tan\phi_1 \tan\phi_2$. The detection probability is then given by

$$P_{10}^\star = 2 \sin^2\phi_1 \sin^2\phi_2 \exp[-\tan\phi_1^2 \tan\phi_2^2]. \tag{15}$$

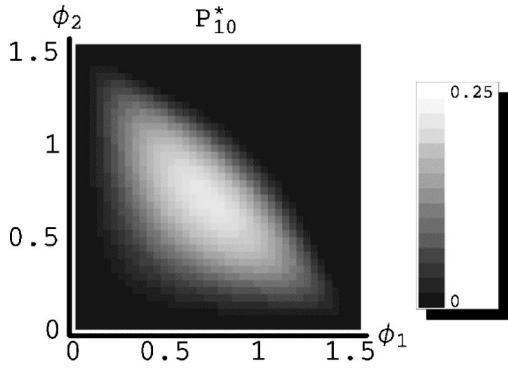


FIG. 2. Density plot of the conditional detection probability P_{10}^* for the preparation of the balanced superposition of Eq. (14). The maximum value ($P_{10}^* \approx 21\%$) is reached for $\phi_1 \equiv \phi_2 \approx 0.715$, corresponding to an optimum amplitude $|\gamma|_{\text{opt}} \approx 0.755$. However, the dependence of the detection probability on ϕ_1 and ϕ_2 is not dramatic, such as is apparent from the plot; there exists a sizeable region in which the detection probability is above $P_{10}^* > 20\%$.

From Eq. (15) we have that $0 < P_{10}^* \leq 0.21$, with the maximum value reached for $\phi_1 \equiv \phi_2 \approx 0.715$, corresponding to an optimum amplitude $|\gamma|_{\text{opt}} \approx 0.755$. However, the dependence of the detection probability on ϕ_1 and ϕ_2 is not dramatic, such that there exists a sizeable region in which the detection probability is above $P_{10}^* > 20\%$ (see Fig. 2). The use of two conditional photodetectors in the present scheme results in a larger detection probability compared to [9] [compare Eq. (15) with Eq. (18) of [9]].

As mentioned above, the symmetric case of a photon detected in the output mode c and no photons in b leads to an equivalent result, up to the replacement $\phi_2 \rightarrow \phi_2 + \pi/2$. In the formula we have

$$P_{01} = e^{-|\gamma|^2} [\sin^2 \phi_1 \cos^2 \phi_2 + |\gamma|^2 \cos^2 \phi_1 \sin^2 \phi_2] \quad (16)$$

and

$$|\psi_{01}\rangle = \frac{\sin \phi_1 \cos \phi_2 |0\rangle - \gamma \cos \phi_1 \sin \phi_2 |1\rangle}{\sqrt{\sin^2 \phi_1 \cos^2 \phi_2 + |\gamma|^2 \cos^2 \phi_1 \sin^2 \phi_2}}. \quad (17)$$

By comparing Eqs. (13) and (17) we also note that the scalar product between the two conditional output states is given by

$$|\langle \psi_{01} | \psi_{10} \rangle|^2 \propto \sin \phi_2 \cos \phi_2 (\sin^2 \phi_1 - |\gamma|^2 \cos^2 \phi_1), \quad (18)$$

which means that for $|\gamma| = \tan \phi_1$, and independently of ϕ_2 , the two states are orthogonal (this also happens for $\phi_2 = p\pi/2, p \in \mathbb{Z}$, and any γ and ϕ_1 , but this case just corresponds to having one state in the vacuum and the other in the one-photon state). In this regime, the scheme provides a reliable source (i.e., with $P_{10} = P_{01} = \exp\{-\tan^2 \phi_1\} \sin^2 \phi_1$, which is larger than 20% in the region around $\phi_1 \approx 0.67$) of a quantum-optical computational basis.

Of course, it is now of interest to study whether or not the superpositions of Eqs. (13) and (17) may be obtained in a realistic implementation of the setup. Since the scheme is based on conditional measurements, the main concern should

be with the photodetection process. Therefore, in the next section we are going to take into account the imperfections of available photodetectors, in order to check the robustness of the preparation scheme against the detectors inefficiency.

III. EFFECTS OF REALISTIC PHOTODETECTION

Light is revealed by exploiting the interaction with atoms or molecules. Each photon ionizes a single atom, and the resulting charge is then amplified to produce a measurable pulse. In practice, however, available photodetectors are hardly performing the ideal measurement of the photon number. Their performances, in fact, are limited by two main kinds of imperfections. On one hand, photodetectors are usually characterized by a quantum efficiency lower than unit, which means that only a fraction of the incoming photons lead to an electric pulse, and ultimately to a ‘‘count.’’ Some photons are either reflected from the surface of the detector, or are absorbed without being transformed into electric pulses. On the other hand, customary photodetectors involve an avalanche process to transform a single ionization event into a recordable pulse. This implies that it is very difficult to discriminate between the presence of a single photon or more than one.

The outcomes from such a detector may be either YES, which means a ‘‘click,’’ corresponding to any number of photons, or NO, which means that no photons have been recorded. This kind measurement is described by a two-value POM,

$$\hat{\Pi}_N = \sum_{p=0}^{\infty} (1 - \eta)^p |p\rangle\langle p|, \quad \hat{\Pi}_Y = \hat{1} - \hat{\Pi}_N, \quad (19)$$

where η is the quantum efficiency and $\hat{1}$ denotes the identity operator. Indeed, for high quantum efficiency (close to unit) $\hat{\Pi}_N$ approaches the projection operator onto the vacuum state, and $\hat{\Pi}_Y$ onto the orthogonal subspace.

The event of observing a click at the PD surveying the output mode b (i.e., D_b , see Fig. 1), and no photons at D_c , is characterized by the probability

$$\begin{aligned} P_{YN}[\eta, \gamma, \phi_1, \phi_2] &= \text{Tr}_{abc} [|\Psi_{\text{OUT}}\rangle\langle\Psi_{\text{OUT}}| \hat{\Pi}_Y \otimes \hat{\Pi}_N] \\ &= e^{-\eta|\gamma|^2 \sin^2 \phi_2} \{1 - e^{-\eta|\gamma|^2 \cos^2 \phi_2} \\ &\quad + \eta \sin^2 \phi_1 [e^{-\eta|\gamma|^2 \cos^2 \phi_2} \\ &\quad + \cos^2 \phi_2 (\eta|\gamma|^2 \sin^2 \phi_2 - 1)]\}. \end{aligned} \quad (20)$$

The corresponding conditional output state is

$$\begin{aligned} \hat{\mathcal{G}}_{YN} &= \frac{1}{P_{YN}} \text{Tr}_{bc} [|\Psi_{\text{OUT}}\rangle\langle\Psi_{\text{OUT}}| \hat{\Pi}_Y \otimes \hat{\Pi}_N] \\ &= \frac{1}{P_{YN}} [d_{00}|0\rangle\langle 0| + d_{11}|1\rangle\langle 1| + d_{01}|0\rangle\langle 1| + d_{01}^*|1\rangle\langle 0|], \end{aligned} \quad (21)$$

where the coefficients are given by (see Appendix A)

$$\begin{aligned} d_{11} &= e^{-\eta|\gamma|^2 \sin^2 \phi_2} \cos^2 \phi_1 [1 - e^{-\eta|\gamma|^2 \cos^2 \phi_2}], \\ d_{00} &= e^{-\eta|\gamma|^2 \sin^2 \phi_2} \sin^2 \phi_1 [1 - (1 - \eta)e^{-\eta|\gamma|^2 \cos^2 \phi_2} \\ &\quad + \eta \cos^2 \phi_2 (\eta|\gamma|^2 \sin^2 \phi_2 - 1)], \\ d_{01} &= e^{-\eta|\gamma|^2 \sin^2 \phi_2} \eta \gamma \sin \phi_1 \sin \phi_2 \cos \phi_1 \cos \phi_2. \end{aligned} \quad (22)$$

In general, the conditional output state $\hat{\rho}_{YN}$ is no longer a pure state. However, as we will see, there are regimes in which $\hat{\rho}_{YN}$ approaches the desired superposition. In order to compare $\hat{\rho}_{YN}$ with the ideal conditional output $|\psi_{10}\rangle$ we consider the fidelity $F = \langle \psi_{10} | \hat{\rho}_{YN} | \psi_{10} \rangle$. From Eqs. (6), (21) and (22) we have

$$\begin{aligned} F[\eta, \gamma, \phi_1, \phi_2] &= \frac{1}{P_{YN}} \\ &\quad \times \frac{e^{-\eta|\gamma|^2 \sin^2 \phi_2}}{\sin^2 \phi_1 \sin^2 \phi_2 + |\gamma|^2 \cos^2 \phi_1 \cos^2 \phi_2} \\ &\quad \times \{ |\gamma|^2 \cos^4 \phi_1 \sin^2 \phi_2 (1 - e^{-\eta|\gamma|^2 \cos^2 \phi_2}) \\ &\quad + 2\eta|\gamma|^2 \sin^2 \phi_1 \sin^2 \phi_2 \cos^2 \phi_1 \cos^2 \phi_2 \\ &\quad + \sin^4 \phi_1 \sin^2 \phi_2 [1 - (1 - \eta)e^{-\eta|\gamma|^2 \cos^2 \phi_2} \\ &\quad + \eta \cos^2 \phi_2 (\eta|\gamma|^2 \sin^2 \phi_2 - 1)] \}. \end{aligned} \quad (23)$$

Our goal is now to find regimes in which the fidelity of the conditional output state is close to unit and, at the same time,

the corresponding detection probability P_{YN} does not vanish. In particular, we are interested in the preparation of those superpositions where the amplitudes of the two components are of the same order, thus assuring that the state is far from being just the vacuum or the one-photon state. This requirement roughly corresponds to the condition

$$\sin \phi_1 \sin \phi_2 \approx \cos \phi_1 \cos \phi_2, \quad (24)$$

whereas a fine tuning of the amplitude, as well as the phase of the superposition, may be obtained by varying the complex amplitude γ of the coherent input. The condition in Eq. (24) is satisfied by two different working regimes of the setup, i.e., by two different pairs of values of the internal phase shifts. These are the balanced choice $\phi_1 = \phi_2 = \pi/4$ and the unbalanced one $\phi_1 \approx 0$, $\phi_2 \approx \pi/2 - \phi_1$, respectively. In both cases, the general expression for the fidelity in Eq. (23) may be considerably simplified, and the corresponding working regime discussed with some details.

A. The case $\phi_1 = \phi_2 = \pi/4$

In the case $\phi_1 = \phi_2 = \pi/4$, the detection probability is rewritten as

$$\begin{aligned} P_{YN}[\eta, \gamma, \pi/4, \pi/4] &= e^{-(1/2)\eta|\gamma|^2} \left\{ 1 - e^{-(1/2)\eta|\gamma|^2} \right. \\ &\quad \left. + \frac{1}{2}\eta \left[e^{(1/2)\eta|\gamma|^2} + \frac{1}{4}(\eta|\gamma|^2 - 2) \right] \right\}, \end{aligned} \quad (25)$$

and the fidelity

$$F[\eta, \gamma, \pi/4, \pi/4] = \frac{[4 - 2\eta + |\gamma|^2(2 + \eta)^2] - 4e^{-(1/2)\eta|\gamma|^2}(1 - \eta + |\gamma|^2)}{(1 + |\gamma|^2)[8 + \eta(\eta|\gamma|^2 - 2) - 4e^{-\eta|\gamma|^2/2}(2 - \eta)]}. \quad (26)$$

The detection probability shows relatively large values ($P_{YN} \geq 50\%$) in a sizeable region (see Fig. 3) of the $\eta - |\gamma|$ space, including also situations with low quantum efficiency. Unfortunately, the fidelity of Eq. (26) is a rapidly decreasing function of the coherent amplitude and, in the relevant region $0 < |\gamma|^2 \lesssim 4$, it is bounded by

$$F_{\text{MAX}} < \frac{2 + |\gamma|^2(9 - 4e^{-|\gamma|^2/2})}{(1 + |\gamma|^2)(|\gamma|^2 + 6 - 4e^{-|\gamma|^2/2})}. \quad (27)$$

This working regime is thus effective only for $|\gamma| \ll 1$, corresponding to the preparation of superposition where the vacuum component is preponderant. Indeed, for balanced superpositions ($|\gamma| \approx 1$) we have the bound $F \lesssim 93\%$. As we will see in the following, this limitation can be overcome by the unbalanced tuning of the internal phase shifts.

Our analysis of the balanced scheme led to conclusions that are in contrast with those of Ref. [10], where, as mentioned in Sec. II, a formally equivalent scheme has been used. The reason for this disagreement stays in the different models employed to describe the photodetection process (see Appendix B). Actually, as far as we know, the YES/NO model used here is more realistic than the photcounter model used there, as, in fact, no evidence of detectors capable of discriminating between the number of incoming photons has been reported. We should conclude that the authors' hope of "reasonable insensitivity" to the detectors inefficiency [10] is not yet realized with current technology.

B. The case $\phi_1 \approx 0, \phi_2 \approx \pi/2 - \phi_1$

In the case $\phi_1 \approx 0, \phi_2 \approx \pi/2 - \phi_1$, the detection probability is given by

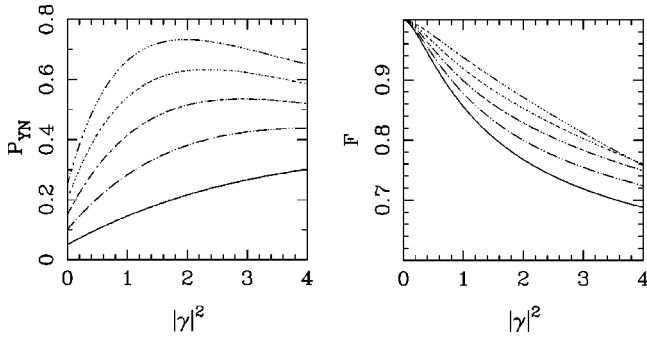


FIG. 3. Performances of the setup with a realistic description of the photodetectors: the case of balanced choice for the internal phase shifts. The figure shows the detection probability P_{10} (on the left) and fidelity F to the desired superposition (on the right) as a function of the intensity of the input coherent state for different values of the quantum efficiency of the photodetectors. In both plots we have, from bottom to top, $\eta=20\%$ (solid line), 40% , 60% , 80% , and 100% .

$$\begin{aligned} P_{YN}[\eta, \gamma, \phi_1=0, \phi_2=\pi/2-\phi_1] \\ \approx e^{-\eta|\gamma|^2} [\eta|\gamma|^2 \cos^2 \phi_2 + \eta \sin^2 \phi_1] \\ \approx \eta \phi_1^2 (1 + |\gamma|^2) \exp[-\eta|\gamma|^2], \end{aligned} \quad (28)$$

and the fidelity

$$F[\eta, \gamma, \phi_1=0, \phi_2=\pi/2-\phi_1] \approx 1 - \frac{1}{2} \phi_1^2 (2 - \eta). \quad (29)$$

Remarkably, the fidelity is now independent of the amplitude of the coherent input, and can be made arbitrarily close to unity by choosing a smaller value for ϕ_1 . The price to pay for this result is a lower value of the detection probability, namely a lower efficiency of the preparation scheme. However, the resulting probability is still large enough to make the scheme an effective source of superposition states. As an example, let us consider ϕ_1 such that $\sin^2 \phi_1 = \cos^2 \phi_2 \approx 0.01$. In this case, we obtain a very high value of the fidelity $F > 99\%$, and yet a detection probability given by $P_{YN} \approx 1\%$ (almost independently of the quantum efficiency). More generally, we can substitute Eq. (28) in Eq. (29) to write

$$F \approx 1 - \frac{2 - \eta}{2\eta(1 + |\gamma|^2)} e^{\eta|\gamma|^2} P_{YN}. \quad (30)$$

Equations (28), (29), and (30) assure that a reliable generation of the desired superposition is achievable (with nonvanishing probability) also for low quantum efficiency at photodetectors.

C. Balanced superpositions

We end the section by illustrating the performance of the setup in preparing the special class of *exactly* balanced superpositions of Eq. (14). The requirement for equal amplitudes reads $|\gamma| = \tan \phi_1 \tan \phi_2$. By substitution in Eqs. (20) and (21) we obtain the detection probability and the corresponding conditional output state. We do not show here the

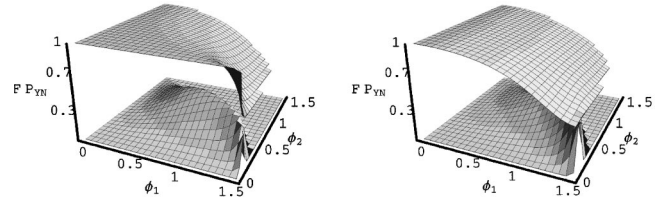


FIG. 4. Performances of the setup with a realistic description of the photodetectors: preparation of balanced superpositions. The figure shows the detection probability P_{10} and the fidelity F to the desired superposition as a function of the internal phase shifts ϕ_1 and ϕ_2 for unit quantum efficiency (on the left) and for $\eta=50\%$ (on the right).

resulting expressions, which are rather cumbersome. Instead, in Fig. 4, we report the behavior of both the fidelity and the detection probability, as a function of the internal phase shifts for two values of the quantum efficiency at the photodetectors. As is apparent from the plots, there always exists a region in which the fidelity is very close to unity and yet the detection probability is larger than 10% . Therefore, for balanced superpositions, the performances with realistic detectors do not substantially differ from that obtained in the ideal working regime discussed in Sec. II.

IV. DISCUSSION AND CONCLUSION

In this paper we presented a method to prepare superposition of the vacuum and one-photon states, which is based on linear optical components and conditional photodetection. Recently, two papers [9,10] appeared on similar subjects and a comparison is in order. In Ref. [10] a scheme to implement the so-called optical state truncation of a coherent state has been proposed, which, in turn, is used to prepare superpositions. In Ref. [9] a scheme based on the alternate application of coherent displacement and a creation operator has been suggested, which is suitable for preparing any truncated single-mode state of the field when a set of N (N being the Fock space truncation dimension) conditional detectors registers no photons.

The main difference of the present scheme when compared with that of the above papers is twofold. On one hand, here an interferometric setup is employed, whereas in both the above papers a set of beam splitters has been used. Interferometric schemes have some advantages in preparing any desired superposition of the vacuum and one-photon states. In fact, for a precise determination of the conditional amplitudes, a precise knowledge of the transmissivity parameters is needed, and moreover, one should be able to tune their values accurately. This can be easily done in an interferometric setup (since it corresponds to vary the internal phase shifts), which is also balanced by construction and therefore robust to losses in the constituent optical elements [12]. On the contrary, tuning at will the transmissivity of a beam splitter is a difficult task. Moreover, in this case fluctuations cannot be balanced. A specific advantage of the present scheme when compared to that of [9] is the use of two conditional photodetectors, which results in a larger

overall detection probability, i.e., a greater efficiency of the preparation process.

The second difference is more relevant, since the aim of any preparation scheme is to be realistically implemented in a laboratory. Indeed, we took into account the imperfections of realistic photodetectors, and we study in detail their effects on the preparation of the superposition. In Ref. [9] only the ideal case of perfect photodetection has been considered, whereas the photocounter model used in Ref. [10] cannot be considered a realistic treatment, since no detectors capable of reliably discriminating between the number of incoming photons are currently implemented.

A further point to be discussed concerns the detection of the qubit. In fact, in order to read out information from an optical qubit we have to discriminate between the vacuum and the presence of a photon. This issue is also of interest for conditional detection schemes by themselves (as the present paper and Refs. [9,10]) and for experiments involving the measurement of coincidence rates. As a matter of fact, avalanche photodetectors are characterized by an active time window in which they are ready to register, with a given quantum efficiency, the arrival (or not) of a photon. In order to reveal the qubit, this time window should be matched with the duration of the optical pulse carrying the information. Any mismatch results in the detector not “seeing” the entire pulse, and therefore in a reduced detection probability. However, the present scheme is robust to this kind of mismatch, since it only corresponds to a reduced quantum efficiency of the YES/NO photodetection process.

In conclusion, we have analyzed a linear, conditional, interferometric setup to prepare any chosen superposition $a_0|0\rangle + a_1|1\rangle$ of the vacuum and one-photon states. It consists of a three-port double interferometer fed by a one-photon state and a coherent state. The scheme involves only linear optical elements and avalanche photodetectors, and therefore should be of interest from the point of view of the experimental realization. In principle, i.e., in the case of a perfect photodetection process, the setup can be used to generate any chosen superposition with a conditional probability about 20%. The imperfections of photodetectors have been taken into account, and their effects have been analyzed in detail. An optimal working regime has been found, in which output states arbitrarily close to the desired superposition are obtained with nonvanishing conditional probability. Typical values for the fidelity are above $F \geq 99\%$, with conditional probability about $P \approx 1\%$. For the relevant case of balanced superposition, the detection probability may be increased by a fine-tuning of the amplitude of the coherent input. In this case, the performances of the setup are approaching the ideal working regime.

V. ACKNOWLEDGMENTS

This work has been cosponsored by CNR and NATO. The author thanks Peter Knight and Martin Plenio for their kind hospitality at Imperial College.

APPENDIX A: CONDITIONAL DENSITY MATRIX FOR REALISTIC PHOTODETECTION

Starting from Eqs. (6), (8), and (19) we have

$$d_{11} = \cos^2 \phi_1 \langle \beta | \hat{\Pi}_Y | \beta \rangle \langle \delta | \hat{\Pi}_N | \delta \rangle,$$

$$\begin{aligned} d_{00} = & \sin^2 \phi_1 [\sin^2 \phi_2 \langle \beta | b \hat{\Pi}_Y b^\dagger | \beta \rangle \langle \delta | \hat{\Pi}_N | \delta \rangle \\ & + \cos^2 \phi_2 \langle \beta | \hat{\Pi}_Y | \beta \rangle \langle \delta | c \hat{\Pi}_N c^\dagger | \delta \rangle \\ & - \sin \phi_2 \cos \phi_2 (\langle \beta | \hat{\Pi}_Y b^\dagger | \beta \rangle \langle \delta | c \hat{\Pi}_N | \delta \rangle + \langle \beta | b \hat{\Pi}_Y | \beta \rangle \\ & \times \langle \delta | \hat{\Pi}_N c^\dagger | \delta \rangle), \end{aligned} \quad (\text{A1})$$

$$\begin{aligned} d_{01} = & \sin \phi_1 \cos \phi_1 (\sin \phi_2 \langle \beta | \hat{\Pi}_Y b^\dagger | \beta \rangle \langle \delta | \hat{\Pi}_N | \delta \rangle \\ & + \cos \phi_2 \langle \beta | \hat{\Pi}_Y | \beta \rangle \langle \delta | \hat{\Pi}_N c^\dagger | \delta \rangle), \end{aligned}$$

where $\beta = \gamma \cos \phi_2$ and $\delta = \gamma \sin \phi_2$. Let us denote by $|z\rangle$ a generic coherent state with complex amplitude $z \in \mathbb{C}$. Then by using the definition (19) of the POM $\{\hat{\Pi}_N, \hat{\Pi}_Y\}$ we have

$$\begin{aligned} \langle z | \hat{\Pi}_N | z \rangle &= \exp\{-\eta |z|^2\}, \\ \langle z | a \hat{\Pi}_N | z \rangle &= z(1-\eta) \exp\{-\eta |z|^2\}, \end{aligned} \quad (\text{A2})$$

$$\langle z | a \hat{\Pi}_N a^\dagger | z \rangle = (1-\eta)[1 + |z|^2(1-\eta)] \exp\{-\eta |z|^2\},$$

and

$$\begin{aligned} \langle z | \hat{\Pi}_Y | z \rangle &= 1 - \langle z | \hat{\Pi}_N | z \rangle, \\ \langle z | a \hat{\Pi}_Y | z \rangle &= z - \langle z | a \hat{\Pi}_N | z \rangle, \end{aligned} \quad (\text{A3})$$

$$\langle z | a \hat{\Pi}_Y a^\dagger | z \rangle = 1 + |z|^2 - \langle z | a \hat{\Pi}_N a^\dagger | z \rangle.$$

Eventually, upon inserting Eqs. (A2) and (A3) in Eq. (A1), we arrive at the expression (22) for the coefficients of the conditional output state.

APPENDIX B: MODELING DETECTORS AS PHOTOCOUNTERS

By modeling a detector as a photocounter, we assume that it is able to discriminate among pulses of different amplitudes, ideally corresponding to the different number of recorded photons. Actually, the number of “clicks” cannot be the number of incoming photons, as the photocounter is characterized by a nonunit quantum efficiency η . The POM describing the measurement is given by a Bernoulli convolution of the ideal photon-number POM $\hat{\Pi}_n = |n\rangle\langle n|$. In the formula, we have

$$\hat{\Pi}_n^\eta = \sum_{k=n}^{\infty} \eta^n (1-\eta)^{k-n} \binom{k}{n} |k\rangle\langle k|. \quad (\text{B1})$$

Therefore, compared to the picture of detectors as avalanche photodetectors, we have that the operator probability for the vacuum detection is the same, i.e., $\hat{\Pi}_N = \hat{\Pi}_0^\eta$, whereas for the case of a single click

$$\hat{\Pi}_1^\eta = \frac{\eta}{1-\eta} \sum_{k=1}^{\infty} k(1-\eta)^k |k\rangle\langle k|. \quad (\text{B2})$$

Equations (A3) are now transformed into

$$\begin{aligned}
\langle z | \hat{\Pi}_1^\eta | z \rangle &= \eta |z|^2 e^{-\eta |z|^2}, \\
\langle z | a \hat{\Pi}_1^\eta | z \rangle &= \eta |z|^2 e^{-\eta |z|^2} [1 + |z|^2 (1 - \eta)], \\
\langle z | a \hat{\Pi}_1^\eta a^\dagger | z \rangle &= \eta |z|^2 e^{-\eta |z|^2} [1 + 3|z|^2 (1 - \eta) + |z|^4 \\
&\quad \times (1 - \eta)],
\end{aligned} \tag{B3}$$

which leads to a detection probability given by

$$P_{10}^\eta = \eta [\sin^2 \phi_1 \sin^2 \phi_2 + |\gamma|^2 \cos^2 \phi_2 (1 - \eta \sin^2 \phi_1)] \tag{B4}$$

and to a conditional output state whose coefficients are expressed as

$$d_{11} = \eta |\gamma|^2 \cos^2 \phi_1 \cos^2 \phi_2,$$

$$d_{00} = \eta \sin^2 \phi_1 [\sin^2 \phi_2 + |\gamma|^2 (1 - \eta) \cos^2 \phi_2], \tag{B5}$$

$$d_{01} = \eta \sin \phi_1 \sin \phi_2 \cos \phi_1 \cos \phi_2 [1 + 2|\gamma|^2 (1 - \eta) \cos^2 \phi_2].$$

For the balanced setting $\phi_1 = \phi_2 = \pi/4$ we have $P_{10}^\eta = \eta/4 [1 + |\gamma|^2 (2 - \eta)]$ and

$$d_{11} = \frac{|\gamma|^2}{1 + |\gamma|^2 (2 - \eta)}, \tag{B6}$$

$$d_{00} = d_{01} = \frac{1 + |\gamma|^2 (1 - \eta)}{1 + |\gamma|^2 (2 - \eta)}.$$

Finally, the fidelity is given by

$$F[\eta, \gamma] = 1 - \frac{|\gamma|^4 (1 - \eta)}{(1 + |\gamma|^2) [1 + |\gamma|^2 (2 - \eta)]}, \tag{B7}$$

which is the result reported in Ref. [10]. The fidelity of Eq. (B7) varies in the range $5/6 \leq F \leq 1$ as a function of the quantum efficiency at the photodetectors.

-
- [1] See, for example, the special issues J. Mod. Opt. **44** (1997), on quantum state preparation and measurement, and Acta Phys. Slov. **48** (1998), on quantum optics and quantum information.
- [2] D.-G. Welsch, W. Vogel, and T. Opatrny, Prog. Opt. **39**, 65 (1999).
- [3] C.H. Bennett, Phys. Scr. **T76**, 210 (1998).
- [4] D. Boschi, S. Branca, F. De Martini, L. Hardy, and S. Popescu, Phys. Rev. Lett. **80**, 1121 (1998); S.L. Braunstein and H.J. Kimble, *ibid.* **80**, 4656 (1998).
- [5] C.H. Bennett and S.J. Wiesner, Phys. Rev. Lett. **69**, 2881 (1992); K. Mattle, H. Weinfurter, P.G. Kwiat, and A. Zeilinger, *ibid.* **76**, 1895 (1996).
- [6] H. Schmidt and A. Imamoglu, Opt. Lett. **21**, 1936 (1996); L.V. Hau, S.E. Harris, Z. Dutton, and C.H. Behroozi, Nature (London) **397**, 594 (1999); S. Rebić, S.M. Tan, A.S. Parkins, and D.F. Walls, J. Opt. B: Quantum Semiclassical Opt. **1**, 490 (1999).
- [7] J. Krause, M.O. Scully, T. Walther, and H. Walther, Phys. Rev. A **39**, 1915 (1989); M. Koziarowski and S.M. Chumakov, *ibid.* **52**, 4194 (1995); P. Domokos, M. Brune, J. Raimond, and S. Haroche, Eur. Phys. J. D **1**, 1 (1998); Varcoe *et al.*, Nature (London) **403**, 743 (2000).
- [8] G.M. D'Ariano, L. Maccone, M.G.A. Paris, M.F. Sacchi, Phys. Rev. A **61**, 053817 (2000); Acta Phys. Slov. **49**, 659 (1999); Fortschr. Phys. **48**, 671 (2000).
- [9] M. Dakna, J. Clausen, L. Knöll, and D.-G. Welsch, Phys. Rev. A **59**, 1658 (1999).
- [10] D.T. Pegg, L.S. Phillips, and S.M. Barnett, Phys. Rev. Lett. **81**, 1604 (1998).
- [11] M.G.A. Paris, Phys. Rev. A **59**, 1615 (1999).
- [12] L. Mandel and E. Wolf, *Optical Coherence and Quantum Optics* (Cambridge University Press, Cambridge, 1995).